

Technical Notes

TECHNICAL NOTES are short manuscripts describing new developments or important results of a preliminary nature. These Notes should not exceed 2500 words (where a figure or table counts as 200 words). Following informal review by the Editors, they may be published within a few months of the date of receipt. Style requirements are the same as for regular contributions (see inside back cover).

Performance of a Low-Power Cylindrical Hall Thruster

Kurt A. Polzin,^{*} Thomas E. Markusic,[†] Boris J. Stanojević,[‡] and Amado Dehoyos[§]
NASA Marshall Space Flight Center,
Huntsville, Alabama 35812
and
Yevgeny Raitses,[¶] Artem Smirnov,^{**} and Nathaniel J. Fisch^{††}
Princeton Plasma Physics Laboratory,
Princeton, New Jersey 08543

DOI: 10.2514/1.28595

Nomenclature

B , B = magnetic induction, T
 I = discharge current, A
 I_{sp} = specific impulse, s
 \dot{m} = flow rate, sccm
 P = discharge power, W
 V = discharge voltage, V
 μ_e = magnetic moment, J/T

I. Introduction

RECENT mission studies [1,2] have shown that a Hall thruster that operates at relatively constant thrust efficiency (45–55%) over a broad power range (300 W–3 kW) is enabling for deep space science missions when compared with state-of-the-art ion thrusters. Although conventional (annular) Hall thrusters can operate at high thrust efficiency at kilowatt power levels, it is difficult to construct one that operates over a broad power envelope down to $\mathcal{O}(100\text{ W})$ while maintaining relatively high efficiency [3]. Scaling to low power requires a decrease in the thruster channel size and an increase

in the magnetic field strength while holding the dimensionless performance scaling parameters constant [4,5]. Increasing the magnetic field becomes technically challenging because the field can more easily saturate the miniaturized inner components of the magnetic circuit, and scaling down the magnetic circuit leaves very little room for magnetic pole pieces and heat shields. This makes it difficult to arrive at an optimal magnetic field configuration. Nonoptimal fields lead to enhanced power and ion losses that lower efficiency and result in increased heating and erosion of thruster components, particularly the critical inner components comprising the coaxial channel and magnetic circuit. Erosion of the thruster channel is one of the main life-limiting factors in conventional Hall thrusters [4].

An alternative approach to the miniaturization problem that has been demonstrated is embodied in the cylindrical-geometry Hall thruster (CHT) [6], which has recently been further developed especially for low-power applications [7]. Figure 1a shows that the CHT departs from the conventional, purely annular, Hall thruster geometry [4]. In contrast to the conventional annular geometry, in the cylindrical geometry the axial potential distribution is critical for electron confinement. This is because there is a large axial gradient in the magnetic field over the cylindrical part of the channel. The electrons drift both azimuthally around the thruster axis and outwards through the $\mu_e \nabla B$ force. In the absence of an axial potential, the electrons would mirror out of the region of high magnetic field. In the CHT, the axial potential that accelerates ions outwards also plays an important role in confining the electrons within the thruster by counteracting the mirroring effect. In addition to being unlike an annular Hall thruster, the CHT differs from an end Hall thruster [8], which has a purely cylindrical geometry, biased channel walls, and a mostly axial applied magnetic field. This is in contrast to the cylindrical ceramic channel with a short annular region to sustain ionization and produce a magnetic field with a strong radial component in the CHT.

The detailed physics in the discharge channel of the CHT has been extensively studied [6,7,9]. In this Note, we report the measured performance (I_{sp} , thrust, and efficiency) of a cylindrical Hall thruster operating at $\mathcal{O}(100\text{ W})$ input power.

II. Experimental Apparatus

Performance measurements are obtained for a 3-cm Princeton Plasma Physics Laboratory (PPPL) CHT, shown in Fig. 1b. The thruster consists of a boron-nitride ceramic channel, an annular anode, two electromagnet coils, and a magnetic core. The thruster channel is a composite of a shorter annular region and a longer cylindrical region. Gas is injected through the anode into the short annular region of the thruster. The length of the annular region is sized to be greater than the ionization mean free path for xenon. This allows for high ionization of the propellant at the boundary between the annular and cylindrical regions. The electromagnet coils are operated using independently controlled power supplies, and the resulting field topology has a mirrorlike structure near the thruster axis.

The working propellant for these experiments is research-grade xenon gas. The cathode and anode flow rates are independently controlled using two variable 10-sccm MKS flow controllers (calibrated on Xe and controllable to ± 0.1 sccm). A commercial HeatWave Labs HWPES-250 hollow cathode is used in these

Received 27 October 2006; revision received 24 January 2007; accepted for publication 24 February 2007. This material is declared a work of the U.S. Government and is not subject to copyright protection in the United States. Copies of this paper may be made for personal or internal use, on condition that the copier pay the \$10.00 per-copy fee to the Copyright Clearance Center, Inc., 222 Rosewood Drive, Danvers, MA 01923; include the code 0748-4658/07 \$10.00 in correspondence with the CCC.

^{*}Research Scientist, Nuclear Systems Branch, Propulsion Systems Department; kurt.a.polzin@nasa.gov. Member AIAA.

[†]Research Scientist; currently Propulsion Test Manager, Space Exploration Technologies, 1 Rocket Road, McGregor, TX 76657. Member AIAA.

[‡]Research Engineer, Madison Research Corporation, 401 Wynn Drive, Huntsville, AL 35805. Member AIAA.

[§]Summer Research Student; currently Test Engineer, Space Exploration Technologies, 1 Rocket Road, McGregor, TX 76657. Member AIAA.

[¶]Research Physicist, MS17 C-Site L239, P.O. Box 451, Princeton, NJ 08543. Member AIAA.

^{**}Graduate Research Assistant; currently, Physicist, Tri Alpha Energy, Inc., 27211 Burbank, Foothill Ranch, CA 92610. Member AIAA.

^{††}Professor, Astrophysical Sciences Dept., MS30 C-Site T162, P.O. Box 451, Princeton, NJ 08543. Member AIAA.

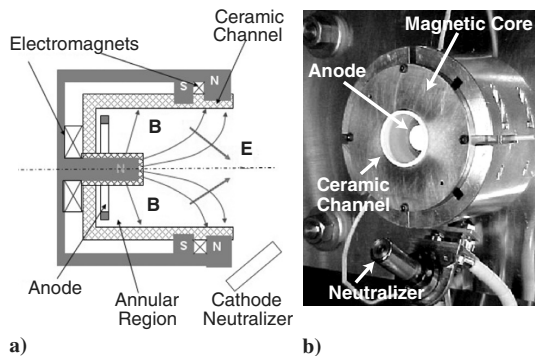


Fig. 1 PPPL cylindrical Hall thruster: a) schematic illustration and b) photograph.

experiments, serving as both the thruster cathode and the neutralizer. In all experiments, the cathode flow rate is 1 sccm. The cathode placement and operation was quite similar to that used in previous testing of the 2.6-cm PPPL CHT [7,9]. The main difference, which did not produce any effect on the discharge characteristics in our testing, is that in the previous experiments the cathode flow rate was typically 2 sccm.

Thrust was measured using the variable-amplitude hanging pendulum with extended-range (VAHPER) thrust stand [10] at the NASA Marshall Space Flight Center (MSFC). This thrust stand employs a unique mechanical linkage system that converts horizontal deflection of the pendulum arm into amplified vertical deflection. The thrust stand is mounted inside a 9-ft-diam, 25-ft-long stainless steel vacuum chamber. The vacuum level inside the chamber is maintained by two 2400 l/s turbopumps and two 9500 l/s cryopumps. The base pressure was 5.7×10^{-7} torr and the background pressure of xenon during thruster operation at ~ 5 sccm total flow rate was $\sim 9 \times 10^{-6}$.

III. Experimental Results and Discussion

Displacement (thrust) calibration of the VAHPER thrust stand is accomplished using an in situ calibration rig that applies a series of known loads normal to the pendulum arm. Calibration can be performed before, during, and after thruster operation. The measured displacement of the vertically deflecting linkage is recorded as the calibration loads are applied to the arm. Assuming that the relationship between the applied force and the measured displacement is linear allows for a linear curve fit of the calibration data found in Fig. 2. The calibration routine propagates the errors associated with the individual force and displacement measurements to accurately account for all systematic errors [11].

Thrust is found by first calculating the linear gap displacement transducer (LGDT) output voltage difference between the steady-state portion of thruster operation and the zero level output immediately following thruster shutdown (see Fig. 3). These data are then converted to thrust using the calibration curve-fit constants found in Fig. 2. Anode efficiency and I_{sp} (specifically, anode I_{sp}) are

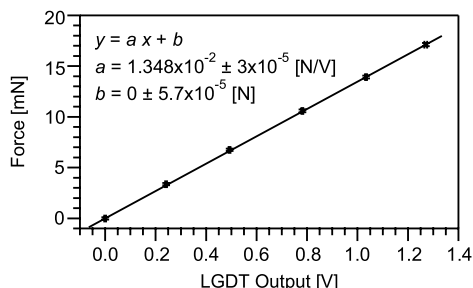


Fig. 2 Applied calibration force plotted as a function of LGDT response. The linear curve is a fit to the displayed data. Error bars on the data points and the fit coefficients represent a 68% (1σ) confidence interval.

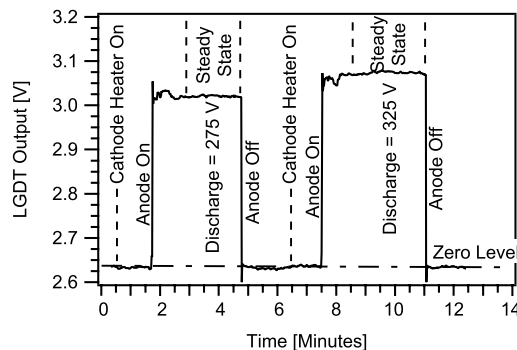


Fig. 3 Raw LGDT output data as a function of elapsed time for two thruster operating points.

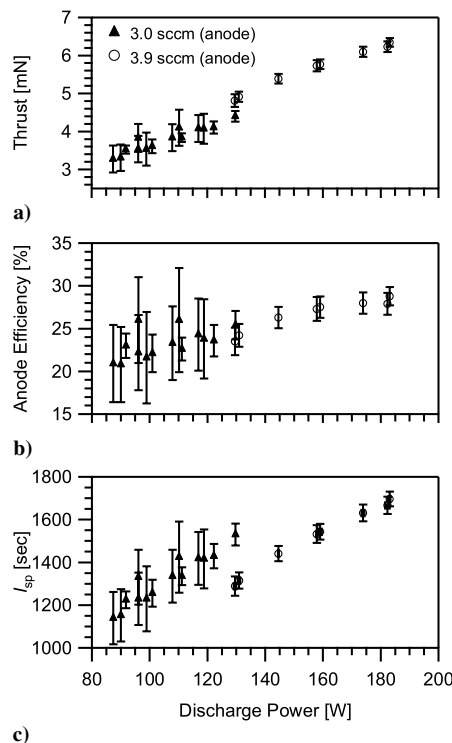


Fig. 4 Performance measurements for a 3-cm cylindrical Hall thruster: a) thrust, b) anode efficiency, and c) I_{sp} as a function of discharge power. The error bars represent a 95% (2σ) confidence interval.

computed according to their standard definitions [12] using recorded anode mass flow rates and power supply outputs. The electromagnet power is not included in the anode efficiency calculation. The uncertainty levels on the performance data represent a 95% (2σ) confidence interval.

Two sets of thrust measurements corresponding to two anode mass flow rates (3 and 3.9 sccm) are presented in Fig. 4a, with the corresponding anode efficiencies plotted in Fig. 4b and I_{sp} values

Table 1 Nominal thruster operating conditions for each of the anode flow rates tested

$\dot{m} = 3$ sccm			$\dot{m} = 3.9$ sccm		
V, V	I, A	P, W	V, V	I, A	P, W
250	0.36	90	250	0.52	130
275	0.36	99	275	0.53	146
300	0.37	111	300	0.53	159
325	0.38	123	325	0.54	176
340	0.38	129	340	0.54	184

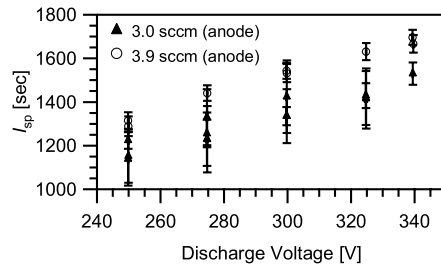


Fig. 5 I_{sp} as a function of discharge voltage. The error bars represent a 95% (2σ) confidence interval.

found in Fig. 4c. These data span a range between 90 to 185 W in discharge power and result in thrust levels between 3 and 6 mN, anode efficiencies between 20 and 27%, and I_{sp} levels between 1100 and 1650 s. For completeness, the voltage, current, and power levels associated with these data are given in Table 1. At the power levels tested, the 3-cm PPPL CHT performance compares favorably with both the SPT-30 [13] and BHT-200 [14] Hall thrusters and is significantly greater than the 6% efficiency and I_{sp} of 850 s measured in a miniaturized conventional (coaxial) Hall thruster at 125-W input power [5]. It is also comparable to previous performance measurements of the 2.6-cm PPPL CHT [7].

In Fig. 4a, thrust increases with discharge power. Anode efficiency (Fig. 4b) also increases with discharge power, going from 20 to 27%. In addition, it appears to asymptote at the higher power levels. Specific impulse (Fig. 4c) increases with discharge power. Additional insight is provided in Fig. 5, in which we see that for a constant mass flow rate, I_{sp} increases with discharge voltage. However, for a given voltage, I_{sp} is greater at the higher mass flow rate. We can speculate that I_{sp} increases due to greater propellant use (i.e., low neutral fraction), the formation of doubly ionized Xe, or a combination of the two. However, we do not have enough information at this time to reach a definite conclusion.

In Fig. 4, we observe that the lower-power data points generally possess much larger errors than the higher-power points. The larger errors are partially attributable to recording of insufficient significant figures in the discharge current measurement for those operating points. The issue was resolved before higher-power testing, but the error had to be conservatively overestimated for the lower-power data set. Additional errors in this lower-power set are due to thermally induced deflections of the vacuum chamber, which occurred as the interior of the building was heated by the sun and warm ambient air and subsequently cooled by the HVAC system, which blew directly onto the vacuum chamber. Both heating and cooling effects were noticeable within minutes and appeared as drifts in the thrust stand position. The heating effects were reduced during the second, higher-power, trial by testing at night and adjusting the HVAC ducts so that they did not blow directly onto the vacuum chamber.

IV. Conclusions

Although conventional (annular) Hall thrusters are efficient in the kilowatt power regime, they become inefficient when scaled down to small sizes. This is due to the difficulties associated with holding the performance scaling parameters constant while decreasing the channel size and increasing the applied magnetic field strength. The cylindrical Hall thruster can be more readily scaled to smaller sizes due to its nonconventional discharge-chamber geometry and associated magnetic field profile.

A series of performance measurements on the 3-cm PPPL CHT over a power ranging from ~85–185 W were performed using the

VAHPER thrust stand. The PPPL CHT produced thrust levels ranging from 3–6 mN, anode efficiencies spanning 20–27%, and I_{sp} between 1100–1650 s. Thrust increased as a function of discharge power, whereas I_{sp} increased with discharge voltage and with increasing anode flow rate.

Acknowledgments

This work was performed under Space Act Agreement NAS8-05791 and supported by the NASA Marshall Space Flight Center (MSFC) Technology Transfer Office. Work performed by the Princeton Plasma Physics Laboratory coauthors were partially supported by the U.S. Air Force Office of Scientific Research. We gratefully acknowledge the contributions of the MSFC technical support staff: Doug Davenport, Tommy Reid, Doug Galloway, Keith Chavers, and Rondal Boutwell. We also extend our gratitude to students Benjamin Spaun, Chris Dodson, and Jeff Gross, and to Freida Lowery in the MSFC Business Development Office.

References

- [1] Manzella, D., Oh, D. Y., and Aadland, R., "Hall Thruster Technology for NASA Science Missions," AIAA Paper 2005-3675, July 2005.
- [2] Witzberger, K. E., and Manzella, D., "Performance of Solar Electric Powered Deep Space Missions Using Hall Thruster Propulsion," AIAA Paper 2005-4268, July 2005.
- [3] Mueller, J., "Thruster Options for Microspacecraft: A Review and Evaluation of State-of-the-Art and Emerging Technologies," *Micropropulsion for Small Spacecraft*, edited by M. M. Micci and A.D. Ketsdever, Vol. 187, Progress in Astronautics and Aeronautics, AIAA, Reston, VA, 2000, pp. 45–137.
- [4] Morozov, A. I., and Savelyev, V. V., "Fundamentals of Stationary Plasma Thruster Theory," *Reviews of Plasma Physics*, edited by B. B. Kadomtsev and V. D. Shafranov, Vol. 21, Consultants Bureau, New York, 2000, p. 203.
- [5] Khayms, V., and Martinez-Sanchez, M., "Fifty-Watt Hall Thruster for Microsatellites," *Micropropulsion for Small Spacecraft*, edited by M. M. Micci and A. D. Ketsdever, Vol. 187, Progress in Astronautics and Aeronautics, AIAA, Reston, VA, 2000, pp. 233–254.
- [6] Raiteses, Y., and Fisch, N. J., "Parametric Investigations of a Nonconventional Hall Thruster," *Physics of Plasmas*, Vol. 8, No. 5, 2001, pp. 2579–2586.
- [7] Smirnov, A., Raiteses, Y., and Fisch, N. J., "Parametric Investigations of a Miniaturized Cylindrical and Annular Hall Thrusters," *Journal of Applied Physics*, Vol. 92, No. 10, 2002, pp. 5673–5679.
- [8] Kaufman, H. R., Robinson, R. S., and Seddon, R. I., "End-Hall Ion Source," *Journal of Vacuum Science and Technology A (Vacuum, Surfaces, and Films)*, Vol. 5, No. 4, 1987, pp. 2081–2084.
- [9] Smirnov, A., Raiteses, Y., and Fisch, N. J., "Plasma Measurements in a 100 W Cylindrical Hall Thruster," *Journal of Applied Physics*, Vol. 95, No. 5, 2004, pp. 2283–2292.
- [10] Polzin, K. A., Markusic, T. E., Stanojev, B. J., DeHoyos, A., and Spaun, B., "Thrust Stand for Electric Propulsion Performance Evaluation," *Review of Scientific Instruments*, Vol. 77, 2006, Article 105108.
- [11] York, D., Evensen, N. M., Martinez, M. L., and Delgado, J. D. B., "Unified Equations for the Slope, Intercept, and Standard Errors of the Best Straight Line," *American Journal of Physics*, Vol. 72, No. 3, 2004, pp. 367–375.
- [12] Jahn, R. G., *Physics of Electric Propulsion*, McGraw-Hill, New York, 1968, pp. 4, 7.
- [13] Jacobson, D. T., and Jankovsky, R. S., "Test Results of a 200 W Class Hall Thruster," AIAA Paper 1998-3792, July 1998.
- [14] Hruby, V., Monheiser, J., Pote, B., Freeman, C., and Connolly, W., "Low Power, Hall Thruster Propulsion System," International Electric Propulsion Conference Paper IEPC-1999-092, Oct. 1999.

R. Myers
Associate Editor